

Determination of total x-ray absorption coefficient using non-resonant x-ray emission

A. J. Achkar¹, T. Z. Regier², E. J. Monkman³, K. M. Shen^{3,4} and D. G. Hawthorn¹

¹*Department of Physics and Astronomy, University of Waterloo, Waterloo, N2L 3G1, Canada*

²*Canadian Light Source, University of Saskatchewan, Saskatoon, Saskatchewan S7N 0X4, Canada*

³*Laboratory of Atomic and Solid State Physics, Department of Physics, Cornell University, Ithaca, NY 14853*

⁴*Kavli Institute at Cornell for Nanoscale Science, Cornell University, Ithaca, NY 14853*

(Dated: February 18, 2022)

An alternative measure of x-ray absorption spectroscopy (XAS) called inverse partial fluorescence yield (IPFY) has recently been developed that, unlike conventional electron yield (EY) and fluorescence yield (FY) measurements, is both bulk sensitive and does not experience saturation or self-absorption effects. In this manuscript, we show that the angle dependence of IPFY can also provide a direct measure of the *total* x-ray absorption coefficient. In contrast, FY and EY measurements are offset or distorted from the total absorption coefficient by an unknown and difficult to measure amount. We demonstrate this technique with test measurements on NiO and NdGaO₃. By measuring the total absorption coefficient, this technique opens the door to using XAS as a non-destructive measure of material composition. In NdGaO₃, we also demonstrate the utility of IPFY for XAS measurements of insulating samples, where neither EY or FY measurements provide reliable data due to sample charging and self-absorption effects, respectively.

PACS numbers: 78.70.Dm,78.70.En,61.05.cj

I. INTRODUCTION

X-ray absorption spectroscopy (XAS) is widely used in biology, the physical sciences and materials engineering as a powerful probe of spatial and electronic structure.¹⁻⁴ In XAS, the by-products of the absorption process, electron yield (EY) and fluorescence yield (FY), are commonly used as measures of the x-ray absorption^{5,6} since transmission experiments often require impractically thin samples. The principle behind EY and FY measurements is that the electron and fluorescence yields bear some proportionality to the absorption coefficient – the number of electrons or photons emitted from decaying atoms in a given thickness of sample is proportional to the number of atoms that are excited. However, the measured FY or EY spectra are not strictly proportional to the total absorption coefficient for several reasons.

First, the thickness of sample probed depends on the relative penetration depth (attenuation length) of the incident photons and the escape depth of the emitted electrons, in the case of electron yield, or photons, in the case of fluorescence yield. The attenuation length can vary over an absorption edge, leading to a distortion of the spectrum, referred to as self-absorption or saturation effects.⁷⁻⁹ Spectra can sometimes be corrected for this self-absorption effect using the angle dependence of the fluorescence.^{7,8} However, this correction procedure can be unreliable since resonant x-ray emission processes¹⁰ that are not accounted for in the self-absorption correction can have a significant influence on the energy dependence of the fluorescence yield.

Second, the magnitude of the EY and FY both depend on the relative probability, ω_{fl} , that an excited atom will decay by emitting photons as opposed to electrons.¹¹ This relative probability differs from atom to atom and edge to edge and is generally not known with great pre-

cision.

Third, the emission is distributed over a range of electron and photon energies. A given detector will not detect all electron or photon energies with equal efficiency. In the case of EY, magnetic or electrostatic fields will also influence the efficiency of detection in the system, which may vary between experiments. In addition, the quantum efficiency of EY (the number of electrons emitted per incident photon) will also vary with photon energy.³ The consequence of all these factors is that the magnitude of the EY or FY signal will generally have a value that is not proportional to the total absorption coefficient but is rather offset or distorted by some often unknown or difficult to calculate factors.

Fortunately, for many applications of XAS, the key features in absorption spectra measured by EY or FY are retained and can still be interpreted to glean important qualitative information about the electronic or spatial structure. However, in many instances, such as correcting for self-absorption effects, calculating resonant scattering cross-sections or determining x-ray penetration depth, it is important to know the absolute value of the absorption coefficient. Moreover, knowing the true value of the absorption coefficient could open the door to using XAS as a quantitative tool for compositional analysis of materials. In principle, the magnitude and energy dependence of the absorption coefficient contains information about the composition of a material in addition to information about the electronic and spatial structure. As the photon energy is increased through an absorption edge, the absorption increases in a step-wise fashion when core electrons are photo-excited with enough energy to enter the continuum of unoccupied states. The magnitude of the edge-step relative to the pre-edge can provide a measure of material composition. This can be determined using tabulated¹² or calculated¹³ values

of the absorption cross-section that are conveniently and freely available online from the Center for X-ray Optics (CXRO) or the National Institute of Standards and Technology (NIST).

With these calculations, the magnitude of the XAS, in particular the edge-step, can be used as a robust quantitative measure of material composition. By fitting the available tabulated or calculated absorption data to the pre- and post-edge of a measured absorption spectrum, one can experimentally derive the stoichiometry of a material in a non-destructive manner. Since they don't measure the total absorption coefficient, FY and EY are not well suited for this type of analysis. Transmission measurements, however, do provide a direct and quantitative measure of the absorption cross-section, but are often impractical since they require ultrathin samples of precisely known thickness (especially in the soft x-ray regime).

Recently, an alternative measure of XAS called inverse partial fluorescence yield (IPFY) has been developed that overcomes the aforementioned shortcomings of EY and FY.¹⁴ Unlike EY and FY measurements, IPFY is both bulk sensitive and free of self-absorption effects. In addition to these properties, we show here in test measurements on NiO and NdGaO₃ that IPFY can reliably obtain a quantitative measure of the total x-ray absorption coefficient, $\mu(E)$, that is not offset, a result that is confirmed by excellent agreement with tabulated or calculated values of the XAS.^{12,13} The ability to derive quantitative information from XAS with IPFY creates new opportunities for chemical speciation and compositional analysis of materials.

In addition, we demonstrate the applicability of IPFY to measurements of strongly insulating samples. In NdGaO₃, neither EY or FY measurements provide a reliable measurement of the XAS of the Nd *M* edge due to strong charging and self-absorption effects respectively. In contrast, IPFY provides excellent agreement with previously measured XAS on Nd metal.

II. EXPERIMENTAL DETAILS

The XAS measurements were performed at the Canadian Light Source's 11-ID SGM beamline. All measurements were made at room temperature. The drain current of the sample provided the electron yield. An energy-dispersive silicon drift detector (SDD) with an energy resolution of ~ 120 eV was used to collect the emission spectra as a function of incident photon energy. The SDD was fixed in position and the sample was rotated about a vertical axis to vary α and β , the angles of incidence and emission, respectively. Dark counts on the detector were negligible. However, a small background in the 200-2000 eV region of the NiO emission spectra was observed, likely due to a slight mis-calibration of the detector electronics. This background potentially introduced an error of up to 20% at the Ni *L*₃ peak and 3% in the post-edge.

The single crystal of cubic NiO was polished to a surface roughness less than 0.03 μm . Its dimensions were 5×5 mm by 0.5 mm thick and it was oriented such that the $\langle 100 \rangle$ direction was perpendicular to the sample surface. The NdGaO₃ single crystal was a 10×10 mm by 0.5mm thick, polished substrate oriented with the $\langle 100 \rangle$ direction perpendicular to the sample surface.

III. INVERSE PARTIAL FLUORESCENCE YIELD

IPFY operates on a different principle than EY or FY, effectively measuring the attenuation length into a sample rather than the number of atoms that are excited and subsequently relax. With IPFY, an energy sensitive detector is used to monitor non-resonant x-ray emission as the incident photon energy is scanned through an absorption edge.¹⁴ This non-resonant (normal) emission may be from a different element or core electron than that associated with the absorption edge under investigation. Monitoring this non-resonant emission provides a measure of the x-ray attenuation length. As the attenuation length decreases through an absorption edge, the same number of atoms are excited (since all photons are absorbed), but fewer of these excitations will correspond to non-resonant transitions. Subsequently, the intensity of the non-resonant emission will dip as the absorption coefficient peaks through an absorption edge. The intensity of the non-resonant emission will also depend on the absorption cross-section of the atom and core-electron corresponding to the non-resonant transition and on the attenuation length of the emitted photons. However, these factors are constant or vary weakly through an absorption edge. As a result, the intensity of the non-resonant emission provides an accurate measure of attenuation length.

The extraction of IPFY from the energy-resolved x-ray emission of NiO is demonstrated in Fig. 1. The x-ray emission of NiO is measured as the incident photon energy, E_i , is scanned through the Ni *L* edge [Fig. 1(a)]. The Ni *L* absorption edge corresponds to exciting a Ni 2*p* electron into unoccupied 3*d* states near the edge (and a continuum of states further above the edge), leaving behind a 2*p* core hole. The emission spectra [Fig. 1(b)] exhibit a peak at emission energy $E_f \sim 840$ eV that corresponds to resonant emission from Ni. This emission is due to the electrons making transitions to fill in the Ni 2*p* core-hole left behind by the Ni *L* edge absorption process. The partial fluorescence yield (PFY) from the Ni 2*p* emission (Fig. 1(c), black curve) suffers significantly from self-absorption effects and bears little resemblance to the absorption coefficient.

In addition to the Ni *L* absorption, the x-ray absorption and emission also have contributions from non-resonant transitions of other core electrons of Ni (3*s*, 3*p*) and from oxygen [the total linear absorption coefficient is the sum of these contributions, $\mu(E_i) = \mu_{Ni}(E_i) +$

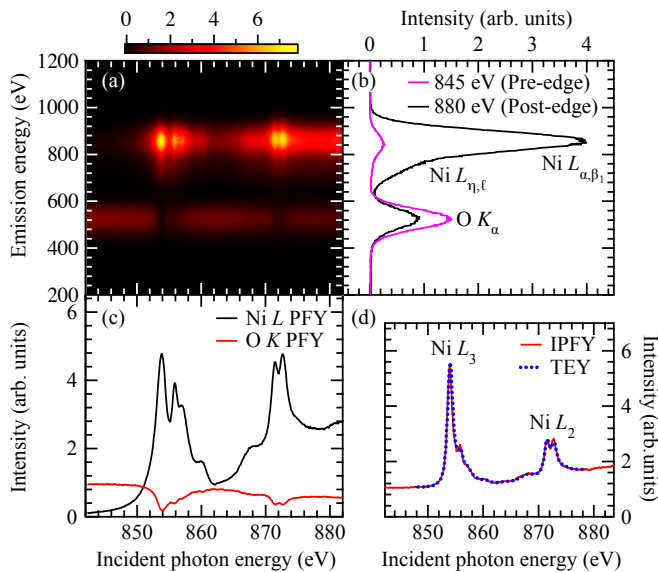


FIG. 1. (Color online) (a) Normalized x-ray fluorescence of NiO as the incident photon energy is scanned through the Ni L_3 and L_2 edges. (b) The emission spectra in the pre- and post-edge regions at incident photon energies of 845 eV and 880 eV taken in 1-eV windows. Emissions corresponding to the resonant Ni $3d$ to $2p$ (L_{α,β_1}) and $3s$ to $2p$ ($L_{\eta,\ell}$) and non-resonant (normal) O $2p$ to $1s$ (K_{α}) processes are observed. (c) The Ni L and O K partial fluorescence yield extracted from panel a in 150-eV wide energy windows centered on the respective emissions. The resonant Ni L PFY shows strong distortions resulting from self-absorption effects. The normal O K PFY dips as the absorption increases through the Ni $L_{2,3}$ absorption edges. (d) The IPFY is the inverse of the O K PFY shown in panel (c). The NiO IPFY is in good agreement with total electron yield data,¹⁵ which has been scaled and offset to match the IPFY.

$\mu_O(E_i)$, where $\mu_{Ni}(E_i) = \mu_{Ni,2p}(E_i) + \mu_{Ni,3s}(E_i) + \mu_{Ni,3p}(E_i) + \dots$ ¹⁶. As shown in Fig. 1(a) and 1(b) there is a band of emission centred at 524 eV corresponding to the non-resonant emission of O $2p$ valence electrons decaying to fill in the O $1s$ core hole (O K emission). The PFY from the O K emission (Fig. 1(c), red curve) exhibits dips at the Ni $L_{2,3}$ absorption edges. The inverse of this spectrum, the IPFY = $1/\text{PFY}_{OK}$, is shown in Fig. 1(d) along with EY measurements of NiO from Ref. 15 that have been scaled and offset to match the IPFY. Similar to previous work¹⁴ on $\text{La}_{1.475}\text{Nd}_{0.4}\text{Sr}_{0.125}\text{CuO}_4$, the agreement between IPFY and EY is very good, highlighting the ability of IPFY to measure the energy dependence of the absorption coefficient of Ni without the strong self-absorption effects experienced by PFY.

It has been shown that the IPFY of thick, homogeneous materials is a function of the total x-ray absorption coefficient $\mu(E_i)$:¹⁴

$$IPFY = \frac{I_0(E_i)}{I(E_i, E_f)} = A(\mu(E_i) + B) \quad (1)$$

where $A = 4\pi/\eta(E_f)\Omega\omega_Y(E_f)\mu_Y(E_i)$ and $B = \mu(E_f)\frac{\sin\alpha}{\sin\beta}$. Here α and β are the angles of incidence and emission, respectively, as measured from the sample surface, $\eta(E_f)$ is the quantum efficiency of the detector at the emission energy, Ω is the detector solid angle, $\mu_Y(E_i)$ is the contribution from the excitation of core electron Y (ex. O $1s$) and $\omega_Y(E_f)$ is the probability of fluorescence at energy E_f resulting from electrons decaying to fill in the core hole left by Y .

In Eq. (1), the constant B is independent of E_i and A depends only weakly on E_i over a narrow energy range and can be treated approximately as constant. This approximation fails over a large energy range, requiring one to correct for the energy dependence of $\mu_Y(E_i)$, as detailed in section IV. As a result, IPFY is proportional to $\mu(E_i)$ plus an offset proportional to B . The crucial feature of Eq. (1) is that the size of the offset B is determined by the geometrical factor $\sin\alpha/\sin\beta$. This allows one to determine $\mu(E_i)$ from experiments with different measurement geometries.

In Fig. 2, we demonstrate that the IPFY of NiO obeys the expected dependence on the sample geometry as detailed in Eq. (1). First, the Ni $L_{2,3}$ PFY spectra measured for various geometries [Fig. 2(a)] depict the strong angle-dependence of self-absorption effects on fluorescence yield (FY) measurements. Notably, attempts to correct the PFY for self-absorption effects using the angle dependence^{7,8} (not shown) do not yield the correct spectra. In contrast, the IPFY spectra measured with the same geometries [Fig. 2(b)] are undistorted and offset from one another, in agreement with Eq. (1). The inset in Fig. 2(b) is a plot of the value of the IPFY spectra at a single value of the incident photon energy [$E_i = 845$ eV (red circles)] as a function of $\sin\alpha/\sin\beta$ for the given experimental geometries. As expected, this offset fits well to a straight line with an intercept equal to $A\mu(845$ eV) and a slope equal to $A\mu(E_f)$. This allows us to subtract $A\mu(E_f)\sin\alpha/\sin\beta$ for each of the spectra. Fig. 2(c) shows the result of these subtractions – the spectra collapse onto a single curve¹⁷. The key point of this analysis is that the resulting spectra, derived entirely by experiment, are directly proportional to the total absorption coefficient without any offsets.

The proportionality to $\mu(E_i)$ is verified by comparing our measurement to tabulated¹² and calculated¹³ values of $\mu(E_i)$. Note, the calculated and tabulated data capture the transitions from the core electron to the continuum, accurately reproducing the edge-step, but do not include the multiplet physics associated with the $2p$ to $3d$ transition. We use the calculated value of the absorption coefficient at the O K emission energy¹⁸ [$\mu(E_f = 524\text{eV}) = 3.14 \times 10^6 \text{ m}^{-1}$ for NiO from Ref. 12] to normalize the subtracted offset and determine the proportionality constant A . The data shown in Fig. 2(c) has been normalized with the appropriate units and is shown along with the tabulated¹² (green curve) and calculated¹³ (red squares) x-ray absorption coefficient. Without oth-

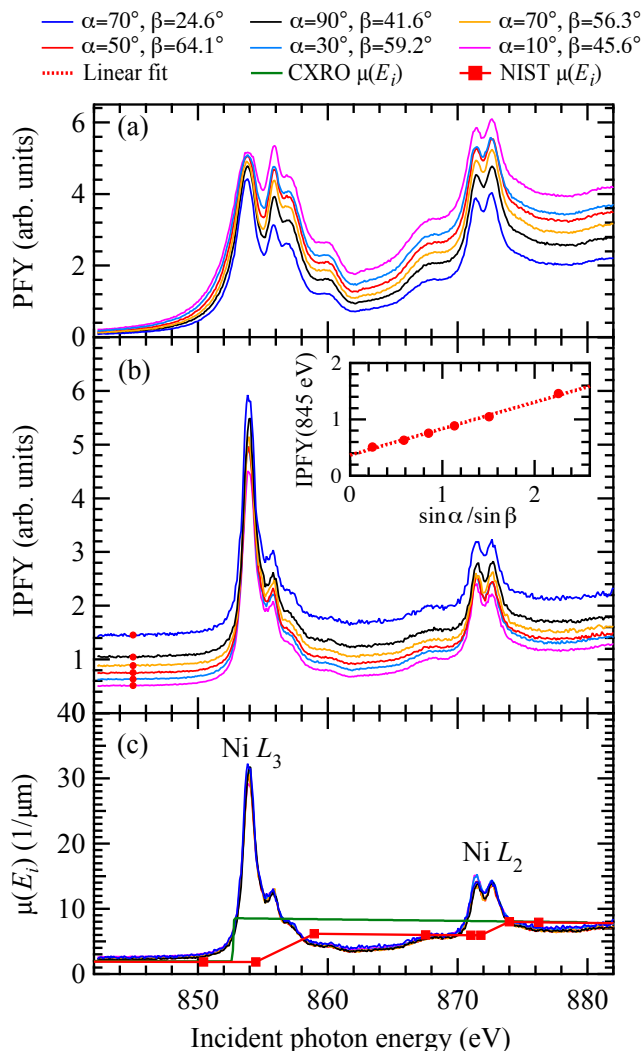


FIG. 2. (Color online) (a) The Ni L PFY for various experimental geometries. The spectra are distorted by strong self-absorption effects that depend on the angle of incidence (α) and angle of emission (β). (b) The IPFY extracted from the O K PFY for the same experimental geometries as panel a. The spectra are offset by a geometry dependent constant, but are otherwise not distorted. The inset plots the IPFY at $E_i = 845$ eV (red circles) as a function of $\sin \alpha / \sin \beta$, which varies linearly as predicted by Eq. (1). (c) The linear absorption coefficient, $\mu(E_i)$, obtained from IPFY spectra. As described in the text, the offsets in the IPFY spectra are subtracted, collapsing the IPFY spectra onto a single curve proportional to $\mu(E_i)$. The spectra are scaled using a single tabulated¹² value for the absorption coefficient of NiO at 524 eV and plotted against the tabulated¹² (green) and calculated¹³ (red squares) absorption coefficients. The magnitude of the edge-jump agrees well with the calculated x-ray absorption in the pre- and post-edge regions.

erwise scaling and offsetting the data, the measured spectra are in excellent agreement with the tabulated coefficients in both the pre- and post-edge regions, demonstrating that IPFY provides a true measure of the total absorption coefficient. In contrast, quantitative analysis of EY or FY measurements require scaling and offsetting data to calculated values of the absorption coefficient above and below the edge.³ This latter procedure requires prior knowledge of the material composition and is subject to uncertainties in the tabulated or calculated values (estimated at 5-20% between 500 and 1000 eV and higher near the absorption edges¹⁹). Moreover, XAS measurements often still have significant structure above an absorption edge (EXAFS) that is not accounted for in the tabulated or calculated values, resulting in additional errors in normalizing data above an absorption edge. In contrast, with IPFY, we obtain the energy dependence of $\mu(E_i)$ directly from measurement and can quantify the data at a single point well below the absorption edge (in the case of NiO at $E_f = 524$ eV). The result of this normalization can be independently checked against the absorption above and below the absorption edge in question and multiple angles can be measured to ensure self-consistency, resulting in a reliable and accurate normalization of the data.

IV. CORRECTION FOR THE ENERGY DEPENDENCE OF $\mu_Y(E_i)$

In the NiO measurements shown above, the described offsetting procedure works well over the narrow energy range covered, giving a quantity approximately proportional to $\mu(E_i)$. However, over a larger energy window, the energy dependence of $\mu_Y(E_i)$ can be significant. An example of this effect is shown in NdGaO₃. In Fig. 3(a), the IPFY measured using the O K emission of NdGaO₃ is shown for three measurement geometries over an extended energy range covering the Nd M edge. The spectra are not rigidly offset, instead appearing to be subject to a sloping background in addition to an offset. This background is due to the energy dependence of $\mu_{OK}(E_i)$ and also to the energy dependence of our measurement of the incident photon flux, I_0 .

In our measurement, and many XAS measurements, I_0 is measured using a Au grid with 85% transmission that is placed between the sample and the last optical component. The total electron yield from the grid, I_{Grid} , is used to measure the incident photon flux. This measurement, however, depends not only on I_0 , but also on the quantum efficiency of the mesh, $\nu(E_i)$ (the number of electrons generated per incident photon), which in general will be energy dependent. As such, $I_{\text{Grid}}(E_i) = I_0\nu(E_i)$

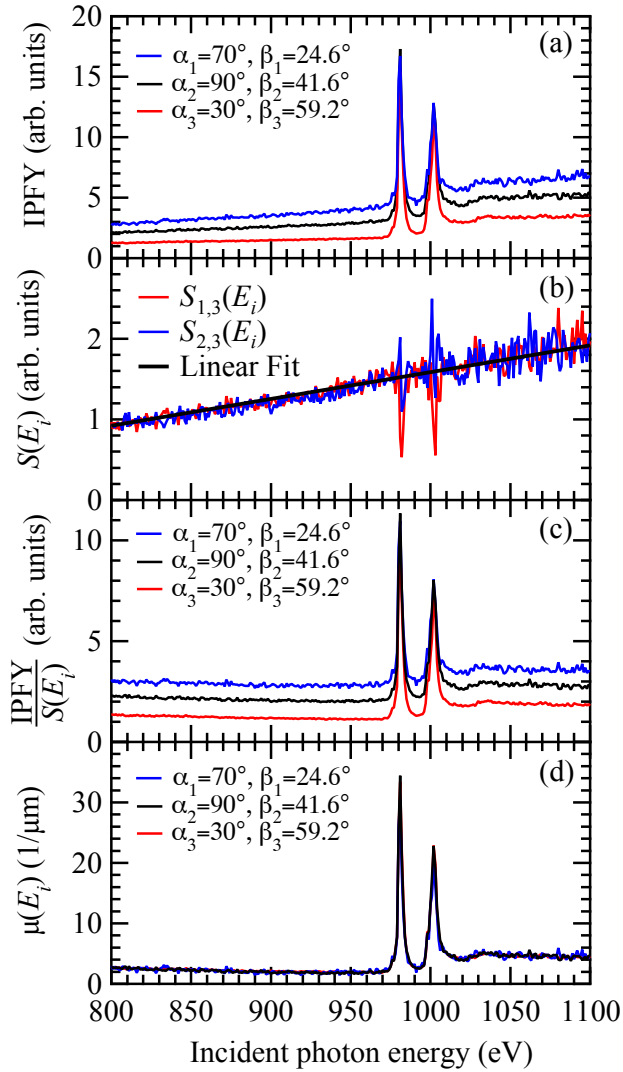


FIG. 3. (Color online) (a) IPFY vs. incident photon energy, E_i , for several measurement geometries. The IPFY is measured using the O K emission in a 150 eV window centered about 524 eV. The measurements at different geometries exhibit different sloping backgrounds due to the energy dependence of $\mu_{OK}(E_i)$ and the quantum efficiency of the I_0 measurement, $\nu(E_i)$. (b) $S(E_i)$ vs. E_i calculated using Eq. (3) with the different measurement geometries depicted in the legend of panel a. The black line is a linear fit to $S(E_i)$. (c) $IPFY(E_i)/S(E_i)$ vs. E_i . The data are rigidly offset by B . (d) The total absorption coefficient, $\mu(E_i)$, vs. E_i determined using Eq. (5) [the data are scaled to $\mu(524 \text{ eV})$ from Ref. 13]. The measurements at different measurement geometries collapse onto a single curve over the whole energy range.

and Eq. (1) should be modified to:

$$IPFY = \frac{I_{\text{Grid}}(E_i)}{I(E_i, E_f)} = \frac{I_0(E_i)\nu(E_i)}{I(E_i, E_f)} \quad (2)$$

$$\approx \frac{D\nu(E_i)}{\mu_Y(E_i)} (\mu(E_i) + B)$$

where $D = A\mu_Y(E_i)$. Fortunately, the energy dependence of both $\nu(E_i)$ and $\mu_Y(E_i)$ can be unambiguously eliminated from the data by subtracting IPFY spectra measured with different measurement geometries and normalizing to the geometry ($\nu(E_i)$ generally also enters into EY and FY measurements, but is typically not corrected for). From Eq. (2) it follows that

$$S_{j,k}(E_i) = \frac{D\nu(E_i)}{\mu_Y(E_i)} \mu(E_f) \quad (3)$$

$$= \frac{IPFY(\alpha_j, \beta_j) - IPFY(\alpha_k, \beta_k)}{\frac{\sin \alpha_j}{\sin \beta_j} - \frac{\sin \alpha_k}{\sin \beta_k}}$$

where j and k correspond to different measurement geometries and $S(E_i)$ is independent of the choice of j and k . We can now write

$$\frac{IPFY}{S(E_i)} = \frac{1}{\mu(E_f)} \left(\mu(E_i) + \mu(E_f) \frac{\sin \alpha}{\sin \beta} \right), \quad (4)$$

which is simply rearranged to yield the total x-ray absorption coefficient:

$$\mu(E_i) = \mu(E_f) \left(\frac{IPFY}{S(E_i)} - \frac{\sin \alpha}{\sin \beta} \right). \quad (5)$$

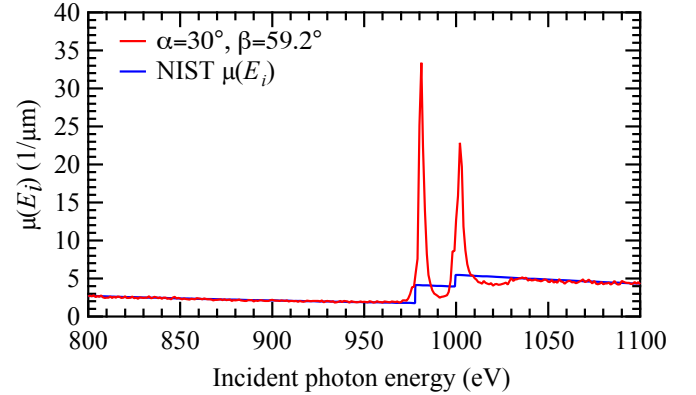


FIG. 4. (Color online) The absorption coefficient of NdGaO₃ extracted from the O K IPFY and corrected for the energy dependence of the O K absorption, $\mu_{O,K}(E_i)$. The incident photon energy was scanned across the Nd M_4 and M_5 edges. The data agrees well with calculated XAS¹³ over a wide energy range.

In Fig. 3, this subtraction is shown, giving $S(E_i)$ that is a smooth function of energy. As shown in Fig. 3(c), dividing the spectra in Fig. 3(a) by $S(E_i)$, provides spectra that are rigidly offset over a wide range in energy. Subtracting $\sin \alpha / \sin \beta$ from the spectra provides $\mu(E_f) / \mu(E_i)$, collapsing the data onto a single curve, as shown in Fig. 3(d). When normalized to the calculated value¹³ of $\mu(524 \text{ eV})$,²⁰ the spectra are in excellent quantitative agreement with the calculated absorption coefficient over a wide energy range above and below the Nd $M_{4,5}$ absorption edge, as shown in Fig. 4.

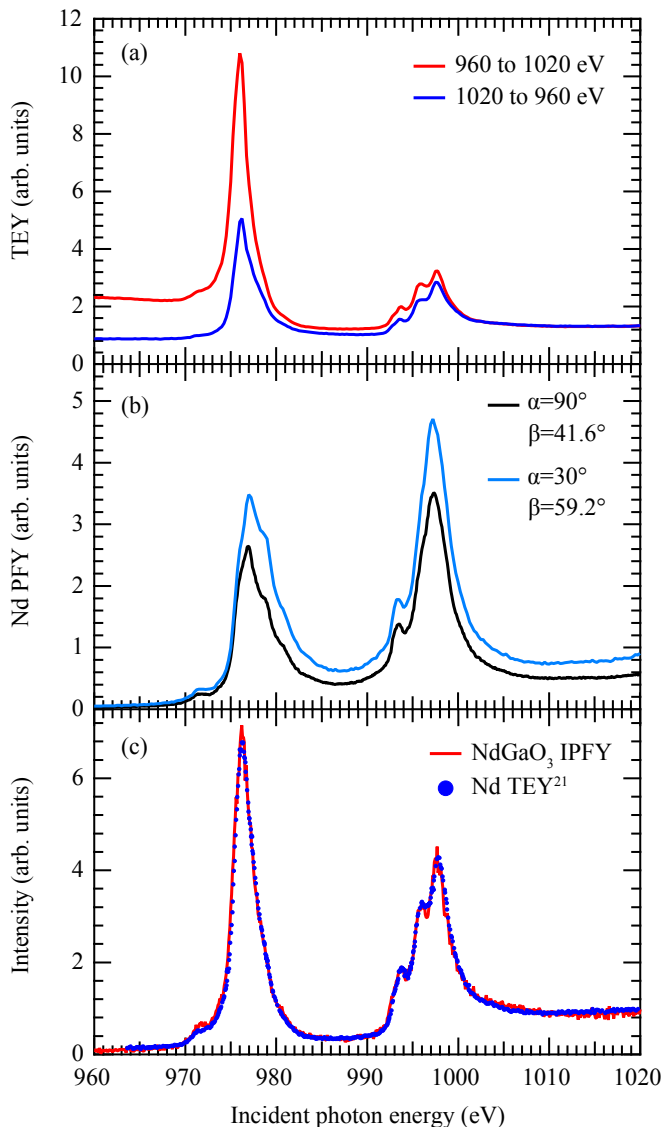


FIG. 5. (Color online) a) The total electron yield of NdGaO_3 exhibits anomalous negative edge-jumps. The spectrum changes dramatically when the incident photon energy is scanned in the negative direction. Both spectra exhibit unusual features and neither match well with TEY on pure metallic Nd.²¹ b) The partial fluorescence yield of Nd is strongly distorted by self-absorption effects. c) The IPFY extracted from the O K PFY of NdGaO_3 agrees extremely well with the TEY of pure Nd,²¹ which is scaled and offset to match the IPFY.

V. IPFY IN STRONG INSULATORS

Finally, we would like to emphasize the role of IPFY to study insulating samples that can be difficult or impossible to measure correctly using FY or EY. An example of such a system is NdGaO_3 . This material is an insulator commonly used as a substrate for oxide film growth. EY measurements of the Nd M edge in NdGaO_3 , shown in

Fig. 5(a), exemplify issues one can encounter when measuring the EY of samples. Here the EY has an unphysical negative edge jump at the absorption edge. The unusual behaviour is attributed to a build-up in positive charge near the surface of the sample that effectively reduces the number of emitted electrons. We were able to reduce the effect by recording the spectra by scanning the incident photon energy in the negative direction (1020 eV to 980 eV) or measuring different spots on the sample, but ultimately these spectra are not reliable.

PFY and TFY in this material are also unreliable. The Nd edge PFY measurements, shown in Fig. 5(b), are heavily distorted by self-absorption effects, similar to NiO. In contrast, the IPFY [Fig. 5(c)] provides the correct XAS spectrum for Nd^{3+} . This is evidenced by excellent agreement with XAS in pure Nd, which like NdGaO_3 has Nd^{3+} character and is described well by atomic multiplet calculations.²¹ In this case, both EY and FY provide erroneous results and transmission measurements are not possible due to the thickness of the material. As such, IPFY provides the only means to measure the correct XAS spectrum. We anticipate IPFY to be widely applicable to similar cases.

VI. DISCUSSION

The fact that the IPFY can be used to determine the complete absorption coefficient will have a significant impact in measurements that require accurate knowledge of the optical constants or atomic scattering form factors, such as modelling of resonant reflectivity or x-ray scattering measurements. Perhaps more significantly, we anticipate that IPFY measurements of the absorption coefficient will be a powerful tool in non-destructive quantitative analysis of material composition, which can be done separately or in conjunction with XANES or EXAFS measurements of electronic and spatial structure. The magnitude of the pre-edge and its relation to the post-edge bears a distinct signature of the quantity of an element relative to the other elements in the material. A simple comparison of the magnitude of the edge-step relative to calculations or to IPFY on similar materials can be used as a clear measure of sample composition. There may also be applications of IPFY to develop standards and refine the calculated and tabulated absorption coefficients,^{12,13} which can vary by up to 20% below 1000 eV.¹⁹

VII. CONCLUSION

We have demonstrated a quantitative measure of the total x-ray absorption coefficient using angle dependent IPFY. Unlike EY or FY, IPFY can provide a measure of the absorption coefficient that is not offset from its true value. We anticipate this technique to have wide applicability in many areas of science and engineering,

potentially opening XAS up to non-destructive, quantitative analysis of material composition.

ACKNOWLEDGMENTS

This research is supported by the Natural Sciences and Engineering Research Council of Canada and by the National Science Foundation through DMR-0847385 and the MRSEC program under DMR-0520404 (Cornell Center for Materials Research). The research described in this paper was performed at the Canadian Light Source, which is supported by NSERC, NRC, CIHR, and the University of Saskatchewan. E.J.M. acknowledges NSERC for PGS support.

-
- ¹ P. Lee, P. Citrin, P. Eisenberger, and B. Kincaid, *Rev. Mod. Phys.*, **53**, 769 (1981).
- ² H. Wende, *Rep. Prog. Phys.*, **67**, 2105 (2004).
- ³ J. Stöhr, *NEXAFS Spectroscopy* (Springer, New York, 1996).
- ⁴ F. deGroot and A. Kotani, *Core Level Spectroscopy of Solids* (CRC Press, Boca Raton, FL, 2008).
- ⁵ W. Gudat and C. Kunz, *Phys. Rev. Lett.*, **29**, 169 (1972).
- ⁶ J. Jaklevic, J. A. Kirby, M. P. Klein, A. S. Robertson, G. S. Brown, and P. Eisenberger, *Solid State Commun.*, **23**, 679 (1977).
- ⁷ L. Tröger, D. Arvanitis, K. Baberschke, H. Michaelis, U. Grimm, and E. Zschech, *Phys. Rev. B*, **46**, 3283 (1992).
- ⁸ S. Eisebitt, T. Böske, J.-E. Rubensson, and W. Eberhardt, *Phys. Rev. B*, **47**, 14103 (1993).
- ⁹ R. Nakajima, J. Stöhr, and Y. U. Idzerda, *Phys. Rev. B*, **59**, 6421 (1999).
- ¹⁰ A. Kotani and S. Shin, *Rev. Mod. Phys.*, **73**, 203 (2001).
- ¹¹ J. Hubbell, P. Trehan, N. Singh, B. Chand, D. Mehta, M. Garg, R. Garg, S. Singh, and S. Puri, *J. Phys. Chem. Ref. Data*, **23**, 339 (1994).
- ¹² B. Henke, E. Gullikson, and J. Davis, *Atomic Data and Nuclear Data Tables*, **54**, 181 (1993).
- ¹³ C. Chantler, *J. Phys. Chem. Ref. Data*, **24**, 71 (1995).
- ¹⁴ A. J. Achkar, T. Z. Regier, H. Wadati, Y.-J. Kim, H. Zhang, and D. G. Hawthorn, *Phys. Rev. B*, **83**, 081106 (2011).
- ¹⁵ M. Abbate, F. M. F. de Groot, J. C. Fuggle, A. Fujimori, Y. Tokura, Y. Fujishima, O. Strebel, M. Domke, G. Kaindl, J. van Elp, B. T. Thole, G. A. Sawatzky, M. Sacchi, and N. Tsuda, *Phys. Rev. B*, **44**, 5419 (1991).
- ¹⁶ J. Yeh and I. Lindau, *At. Data Nucl. Data Tables*, **32**, 1 (1985).
- ¹⁷ There is a slight discrepancy in the peak intensities which is due to a slight magnetic linear dichroism in NiO due to anti-ferromagnetic ordering in the (111) direction.
- ¹⁸ The O *K* emission is primarily from 2*p* valence electrons decaying to fill the 1*s* core hole and is peaked at a photon energy below the absorption threshold.
- ¹⁹ C. Chantler, *J. Phys. Chem. Ref. Data*, **29**, 597 (2000).
- ²⁰ The absorption coefficient from tabulated data¹² and calculations¹³ differ by ~20% at 524 eV. The calculated values provide better agreement with our measurements.
- ²¹ B. T. Thole, G. van der Laan, J. C. Fuggle, G. A. Sawatzky, R. C. Karnatak, and J.-M. Esteve, *Phys. Rev. B*, **32**, 5107 (1985).